NATIONAL ADVISORY COMMITTEE FOR AERONAUTICS

REPORT No. 890

INVESTIGATIONS OF EFFECTS OF SURFACE TEMPERATURE AND SINGLE ROUGHNESS ELEMENTS ON BOUNDARY-LAYER TRANSITION

By HANS W. LIEPMANN and GERTRUDE H. FILA

NAVY RESEARCH SECTION
SCIENCE DIVISION
REFERENCE DEPARTMENT
LIBRARY OF CONGRESS
SEP 1 9 1949

1947

19950825 128

For sale by the Superintendent of Documents, U. S. Government Printing Office, Washington 25, D. C. - - - - - - - - - - - Price 15 cents

DTIC QUALITY INSPECTED 3

19950825 128

DTIC ELECTED AUG 31 1995 F

NATIONAL ADVISORY COMMITTEE FOR AERONAUTICS

REPORT No. 890

INVESTIGATIONS OF EFFECTS OF SURFACE TEMPERATURE AND SINGLE ROUGHNESS ELEMENTS ON BOUNDARY-LAYER TRANSITION

By HANS W. LIEPMANN and GERTRUDE H. FILA

NAVY RESEARCH SECTION
SCIENCE DIVISION
REFERENCE DEPARTMENT
LIBRARY OF CONGRESS
SEP 19 1995

DISTRIBUTION STATEMENT A
Approved for public release;
Distribution Unlimited

1947

For sale by the Superintendent of Documents, U. S. Government Printing Office, Washington 25, D. C. - - Price 15 cents

DTIC QUALITY INSPECTED 5

AERONAUTIC SYMBOLS

1. FUNDAMENTAL AND DERIVED UNITS

	Symbol	Metric		English	
		Unit	Abbreviation	Unit	Abbreviation
Length	l	meter	m	foot (or mile)	ft (or mi)
Time	t	second	s	second (or hour)	sec (or hr)
Force	F	weight of 1 kilogram	kg	weight of 1 pound	lb
Power	P	horsepower (metric)		horsepower	hp
Speed	V	kilometers per hour	kph	miles per hour	mph
		meters per second	mps	feet per second	fps

2. GENERAL SYMBOLS

W Weight$=mg$

g Standard acceleration of gravity$=9.80665$ m/s^2 or 32.1740 ft/sec^2

m Mass$=\frac{W}{g}$

I Moment of inertia$=mk^2$. (Indicate axis of radius of gyration k by proper subscript.)

μ Coefficient of viscosity

ν Kinematic viscosity

ρ Density (mass per unit volume)

Standard density of dry air, 0.12497 kg-m^{-4}-s^2 at 15° C and 760 mm; or 0.002378 lb-ft^{-4} sec^2

Specific weight of "standard" air, 1.2255 kg/m^3 or 0.07651 lb/cu ft

3. AERODYNAMIC SYMBOLS

S Area

S_w Area of wing

G Gap

b Span

c Chord

A Aspect ratio, $\frac{b^2}{S}$

V True air speed

q Dynamic pressure, $\frac{1}{2}\rho V^2$

L Lift, absolute coefficient $C_L=\frac{L}{qS}$

D Drag, absolute coefficient $C_D=\frac{D}{qS}$

D_0 Profile drag, absolute coefficient $C_{D_0}=\frac{D_0}{qS}$

D_i Induced drag, absolute coefficient $C_{D_i}=\frac{D_i}{qS}$

D_p Parasite drag, absolute coefficient $C_{D_p}=\frac{D_p}{qS}$

C Cross-wind force, absolute coefficient $C_C=\frac{C}{qS}$

i_w Angle of setting of wings (relative to thrust line)

i_t Angle of stabilizer setting (relative to thrust line)

Q Resultant moment

Ω Resultant angular velocity

R Reynolds number, $\rho\frac{Vl}{\mu}$ where l is a linear dimension (e.g., for an airfoil of 1.0 ft chord, 100 mph, standard pressure at 15° C, the corresponding Reynolds number is 935,400; or for an airfoil of 1.0 m chord, 100 mps, the corresponding Reynolds number is 6,865,000)

α Angle of attack

ϵ Angle of downwash

α_0 Angle of attack, infinite aspect ratio

α_i Angle of attack, induced

α_a Angle of attack, absolute (measured from zero-lift position)

γ Flight-path angle

REPORT No. 890

INVESTIGATIONS OF EFFECTS OF SURFACE TEMPERATURE AND SINGLE ROUGHNESS ELEMENTS ON BOUNDARY-LAYER TRANSITION

By HANS W. LIEPMANN and GERTRUDE H. FILA

California Institute of Technology

Accesion For
NTIS CRA&I ☑
DTIC TAB ☐
Unannounced ☐
Justification .....
By .....
Distribution /
Availability Codes
Dist | Avail and / or Special
A-1

National Advisory Committee for Aeronautics

Headquarters, 1500 New Hampshire Avenue NW., Washington 25, D. C.

Created by act of Congress approved March 3, 1915, for the supervision and direction of the scientific study of the problems of flight (U. S. Code, title 49, sec. 241). Its membership was increased to 15 by act approved March 2, 1929. The members are appointed by the President, and serve as such without compensation.

JEROME C. HUNSAKER, Sc. D., Cambridge, Mass., *Chairman*

LYMAN J. BRIGGS, Ph. D., *Vice Chairman*, Director, National Bureau of Standards.

CHARLES G. ABBOT, Sc. D., *Vice Chairman, Executive Committee*, Secretary, Smithsonian Institution.

HENRY H. ARNOLD, General, United States Army, Commanding General, Army Air Forces, War Department.

WILLIAM A. M. BURDEN, Assistant Secretary of Commerce for Aeronautics.

VANNEVAR BUSH, Sc. D., Director, Office of Scientific Research and Development, Washington, D. C.

WILLIAM F. DURAND, Ph. D. Stanford University, California.

OLIVER P. ECHOLS, Major General, United States Army, Chief of Matériel, Maintenance, and Distribution, Army Air Forces, War Department.

AUBREY W. FITCH, Vice Admiral, United States Navy, Deputy Chief of Naval Operations (Air), Navy Department.

WILLIAM LITTLEWOOD, M. E., Jackson Heights, Long Island, N. Y.

FRANCIS W. REICHELDERFER, Sc. D., Chief, United States Weather Bureau.

LAWRENCE B. RICHARDSON, Rear Admiral, United States Navy, Assistant Chief, Bureau of Aeronautics, Navy Department.

EDWARD WARNER, Sc. D., Civil Aeronautics Board, Washington, D. C.

ORVILLE WRIGHT, Sc. D., Dayton, Ohio.

THEODORE P. WRIGHT, Sc. D., Administrator of Civil Aeronautics, Department of Commerce.

GEORGE W. LEWIS, Sc. D., *Director of Aeronautical Research*

JOHN F. VICTORY, LL. M., Secretary

HENRY J. E. REID, Sc. D., Engineer-in-Charge, Langley Memorial Aeronautical Laboratory, Langley Field, Va.

SMITH J. DEFRANCE, B. S., Engineer-in-Charge, Ames Aeronautical Laboratory, Moffett Field, Calif.

EDWARD R. SHARP, LL. B., Manager, Aircraft Engine Research Laboratory, Cleveland Airport, Cleveland, Ohio

CARLTON KEMPER, B. S., Executive Engineer, Aircraft Engine Research Laboratory, Cleveland Airport, Cleveland, Ohio

---

TECHNICAL COMMITTEES

AERODYNAMICS

POWER PLANTS FOR AIRCRAFT

AIRCRAFT CONSTRUCTION

OPERATING PROBLEMS

MATERIALS RESEARCH COORDINATION

Coordination of Research Needs of Military and Civil Aviation

Preparation of Research Programs

Allocation of Problems

Prevention of Duplication

LANGLEY MEMORIAL AERONAUTICAL LABORATORY
Langley Field, Va.

AMES AERONAUTICAL LABORATORY
Moffett Field, Calif.

AIRCRAFT ENGINE RESEARCH LABORATORY, Cleveland Airport, Cleveland, Ohio

Conduct, under unified control, for all agencies, of scientific research on the fundamental problems of flight

---

OFFICE OF AERONAUTICAL INTELLIGENCE, Washington, D. C.

Collection, classification, compilation, and dissemination of scientific and technical information on aeronautics

REPORT No. 890

INVESTIGATIONS OF EFFECTS OF SURFACE TEMPERATURE AND SINGLE ROUGHNESS ELEMENTS ON BOUNDARY-LAYER TRANSITION

By Hans W. Liepmann and Gertrude H. Fila

SUMMARY

The laminar boundary layer and the position of the transition point were investigated on a heated flat plate. It was found that the Reynolds number of transition decreases as the temperature of the plate is increased. It is shown from simple qualitative analytical considerations that the effect of variable viscosity in the boundary layer due to the temperature difference produces a velocity profile with an inflection point if the wall temperature is higher than the free-stream temperature. This profile is confirmed by measurements. Furthermore, it is confirmed that, even with large deviation from the Blasius condition, the velocity and temperature profiles are very nearly identical, as predictable theoretically for a Prandtl number σ of the order of 1.0 (for air, $\sigma=0.76$). The instability of inflection-point profiles is discussed.

Studies of the flow in the wake of large, two-dimensional roughness elements are presented. It is shown that a boundary layer can separate and reattach itself to the wall without having transition take place.

INTRODUCTION

The problem of boundary-layer transition has been for several years the subject of research projects sponsored by the National Advisory Committee for Aeronautics. One part of the problem, the question of the stability of laminar flow, can be considered solved. (The problem of laminar instability should not be confused with the problem of predicting transition. For further details, see reference 1.) The experiments carried out at the National Bureau of Standards (reference 2) and at the California Institute of Technology (reference 3) agree very well with the results of Lin in a very complete theoretical analysis of laminar instability (reference 4), and there is no doubt that the laminar boundary layer first becomes unstable with respect to small perturbations at a certain critical Reynolds number R_1.

In the course of the experimental investigations, the effects of external turbulence, curvature, and pressure gradients on boundary-layer transition have been investigated. The present report treats principally investigations of two other factors, the effects of elevated surface temperature and of roughness elements upon the position of the transition point. The investigation of effects of this kind is prompted partially by practical considerations. The effect of roughness elements on transition is a question of obvious importance in connection with laminar-flow airfoils, and the effect of an increased surface temperature on the position of the transition point is of importance in connection with the use of thermal de-icing equipment on low-drag airfoils.

In addition to these practical considerations, both problems are of interest for an understanding of the general mechanism of transition. From the investigation of laminar instability (references 2 to 4), it is clear that certain disturbances will increase in any laminar boundary layer if the Reynolds number exceeds a critical value R_1. The Reynolds number R_2 at which transition actually begins can be defined in a way which makes it possible to link R_2 to R_1 (reference 1). A rough estimate shows that, as in known from experimental evidence, R_2 can be quite large compared with R_1. The difference between R_2 and R_1 depends upon the magnitude of the initial disturbances, for example, the external turbulence level, and upon the amount of amplification in the instability zone for this particular disturbance. For a given Reynolds number, the amount of amplification depends upon the shape of the mean-velocity profile.

Small roughness elements introduce disturbances into the laminar layer and thus precipitate transition. For example, regularly spaced small roughness elements can be used to introduce regular oscillations in the laminar boundary layer (reference 3). If the height of the elements is small compared with the boundary-layer thickness, there is no change in the mean-velocity profile and, therefore, no change in the amplification zone. Most earlier work on the influence of roughness on transition was concerned with investigations of uniformly distributed small roughness elements. (See, e. g., reference 5.) The measurements presented in the present report, however, are concerned with single, large, two-dimensional elements. The flow in the wake of a single roughness element is studied.

It should be noted that the flow in the wake of a single large roughness element in the boundary layer bears some similarity to the flow which exists on the upper surface near the leading edge of an airfoil at an angle of attack. The boundary-layer flow from the stagnation point around the nose of the airfoil is essentially similar to flow along a surface with a large roughness element (fig. 1). In fact, it is this effect—namely, the separation of a boundary layer from the wall and possible subsequent reattachment to the wall—which was of primary interest in the roughness study.

It is a well-known fact (e. g., reference 3) that a "free" laminar boundary layer becomes turbulent at a much lower Reynolds number than a normal "wall" boundary layer. Another important question, therefore, is whether the (laminar) separated layer becomes turbulent before reattach-

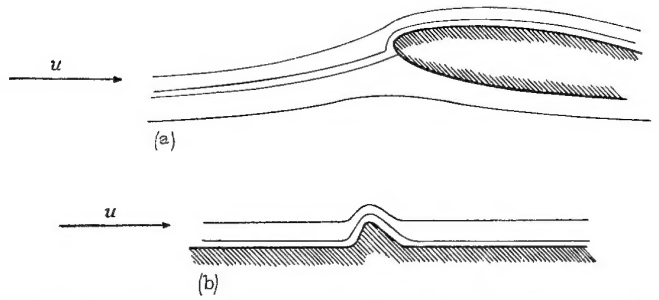

(a) Boundary-layer flow from the stagnation point around the nose of an airfoil at a small angle of attack.
(b) Boundary-layer flow along a surface with a large, single roughness element.

FIGURE 1.—Similarity of flow near the sharp leading edge of an airfoil and over a roughness element on a flat plate.

ment to the wall or whether it is possible for the layer to remain laminar through the period of reattachment. This investigation was prompted by some previous interesting results on similar roughness elements (reference 3).

The surface temperature affects the position of the transition point in two distinctly different ways. One is essentially an effect of gravitational forces and is due to the density differences in the boundary layer; the other effect is due to the dependence of the viscosity of the fluid upon its temperature, which results in a change in the mean-velocity profile. The first effect has been discussed by Prandtl (reference 6) and Schlichting (reference 7) and was experimentally investigated by Reichardt (reference 8). This effect is due to the fact that for a stable configuration in a gravity field the density gradient should be directed downward (i.e., the denser fluid should be below). Thus air flow above a horizontal heated plate is destabilized, since the layers close to the plate have a higher temperature and a lower density. (A hot stream past a cold plate in the same configuration is stabilized.) The second effect was noted by Frick and McCullough (reference 9), who investigated the effects of internal heating, for the purpose of preventing formation of ice, on the characteristics of low-drag airfoils. The viscosity of a gas increases with increasing temperature. In laminar flow, as is shown later from the equation of motion, an increase in the wall temperature causes a negative viscosity gradient outward from the heated surface, which causes the appearance of inflection points in the boundary-layer profiles. The instability of inflection-point profiles is known (reference 4) to be larger than that of profiles with negative curvature throughout, and transition is thus hastened. This transition is the effect investigated in the present set of measurements.

This investigation was conducted at the California Institute of Technology under the sponsorship and with the financial assistance of the National Advisory Committee for Aeronautics. Dr. C. B. Millikan supervised the research. The authors wish to acknowledge the contribution of Mr. P. O. Johnson, who carried out the measurements on the roughness problem and designed the heated-plate unit. Discussions with Messrs. J. Laufer and S. Corrsin were very helpful.

SYMBOLS

x	distance along surface of plate from leading edge
y	distance perpendicular from surface of pla
U,V	local mean velocity in x- and y-direction respectively
U_0	mean velocity of free stream in x-direction
u	x-component of velocity fluctuations
$\frac{u'}{U}=\sqrt{\frac{\overline{u^2}}{U^2}}$	root-mean-square of u-velocity fluctuati level
ρ	density
μ	absolute viscosity
$q=\frac{1}{2}\rho U_0^2$	dynamic pressure of free stream
p	static pressure
$\nu=\frac{\mu}{\rho}$	kinematic viscosity
$\eta=y\sqrt{\frac{U_0}{\nu x}}$	Blasius nondimensional parameter
t	time
$R=\frac{U_0 x}{\nu}$	Reynolds number using the parameter x
R_1	Reynolds number corresponding to low limit of stability
R_2	Reynolds number corresponding to begi ning of transition
x_2	distance along surface of plate to beginni of transition
T	temperature, ° C
θ	temperature difference between wire a air, ° C
$\theta_u=T_u-T_f$	temperature difference between a point the boundary layer and in the free strea ° C
$\theta_w=T_w-T_f$	temperature difference between wall and fr stream, ° C
$\sigma=\frac{\nu}{k}$	Prandtl number
ϵ	height of roughness element, inches
d	diameter of two-dimensional roughness el ment, inches
x_0	distance of roughness element from leadi edge of plate
H	rate of heat loss of hot wire to air
A, B	hot-wire constants
α	temperature coefficient of resistance of wi
r	resistance of wire when heated to tempe ature T
r_0	resistance of wire at temperature of 0° C
r_f	resistance of unheated wire at temperatu T_f in free stream
r_u	resistance of unheated wire at temperatu T_u at any point in heated boundary lay
r_w	resistance of unheated wire at temperatu T_w at heated wall
i	heating current of wire
Subscripts:	
w	wall
f	free stream
u	point in heated boundary layer

APPARATUS AND METHODS

WIND TUNNEL AND PLATE INSTALLATION

The wind tunnel used for this investigation was constructed at the California Institute of Technology in 1938. is of the Eiffel type with a 16–to–1 contraction ratio. he working section is 20 inches square and 12 feet long, nd is provided with adjustable side walls to facilitate btaining a constant velocity along its entire length. The ower unit is a 5-horsepower direct-current motor driving two-blade wooden fan 30 inches in diameter. A sketch of ie tunnel is shown in figure 2 (a).

A polished aluminum plate ¼ inch thick and 19 inches ide was used for this work. The plate was 6 feet long and ie leading edge was beveled to a sharp edge.

The plate was mounted vertically in the center of the ind tunnel on built-up grooves as shown in figure 2 (b). he upper surface of the tunnel is removable in panels; ius adjustment of the upper edge of the plate to obtain a ertical plate was facilitated. The observation panel is -inch plate glass located on the upper tunnel surface and is nterchangeable with any of the removable panels. The oughness elements used in this investigation were wooden alf-circular cylinders mounted on the plate as shown in gure 2 (c).

The heating elements for the heated-plate experiments ere mounted on the back of the plate, placed between two in sheets of asbestos, and further insulated with cork acking. This arrangement resulted in a test plate of 1½- ch thickness and thus necessitated adjustment of other hysical factors in the tunnel to simulate flat-plate flow. The method used to accomplish this adjustment is discussed later in the report. The plate was heated from the leading edge to $x=75$ centimeters. Figure 3 shows the test plate mounted in the test section of the wind tunnel.

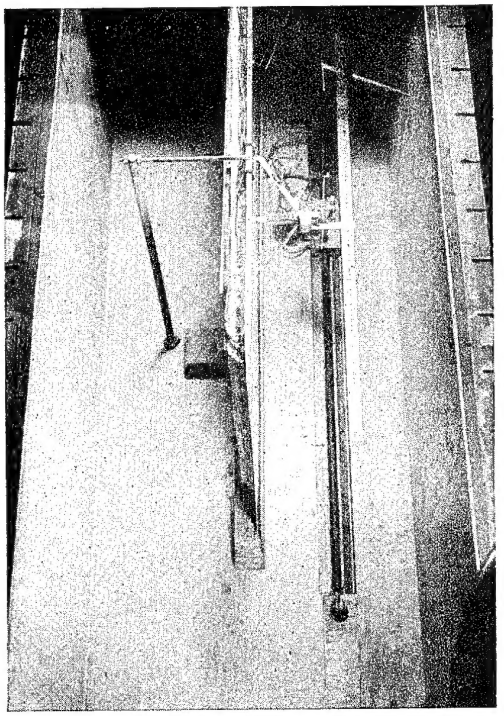

FIGURE 3.—Test plate mounted in working section of wind tunnel with top panels removed. Photograph taken from above and upstream.

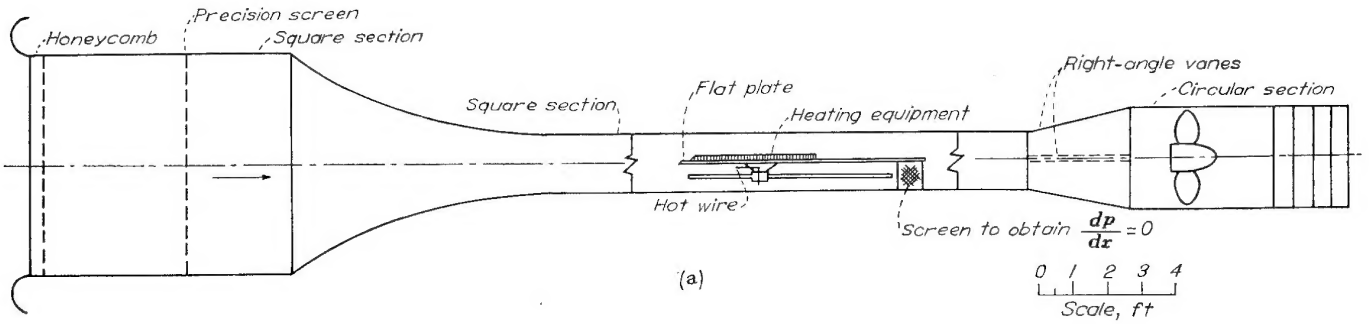

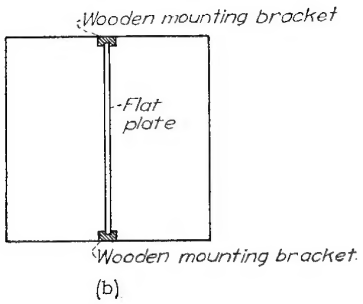

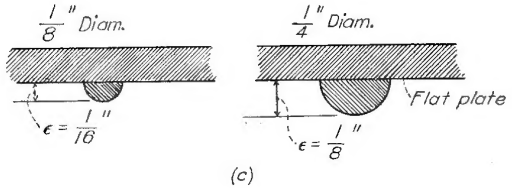

(a) Schematic diagram of the wind tunnel. Top view. (b) Mounting of flat plate. Not to scale. (c) Mounting of roughness elements. Not to scale.

FIGURE 2.—Wind tunnel and plate installation.

DESCRIPTION OF HOT-WIRE EQUIPMENT

The hot-wire technique has been used extensively at the California Institute of Technology, and its use has been continued in these investigations. All measurements of velocity fluctuations were made with the hot-wire apparatus, and most of the velocity profiles were obtained by this method. (A hypodermic-needle total-head tube was used to verify the hot-wire results obtained when investigating the velocity distribution of the boundary layer on a heated plate.) The determination of the transition point was made by means of a hot-wire anemometer and an oscilloscope.

The hot wire.—The hot wire used in these experiments was constructed of copper lead-in wires, ceramic tubing, fine sewing needles, and platinum wires 0.0005 and 0.00024 inch in diameter for mean-speed and velocity-fluctuation measurements, respectively. Two copper wires were thrust through small holes in a 4-inch length of ceramic tubing for mean-speed measurements and measurements of the fluctuations parallel to the mean flow. These wires were cemented into the tubing at both ends, and needles were soldered to them. The platinum hot wire was then soft-soldered across the tips of the sewing needles. (The silver cover of the 0.00024-inch Wollaston wire was removed by immersion in nitric acid before the wire was soldered to the needles.)

The 0.0005-inch wires used for measuring mean speed were generally about 3 millimeters long. Velocity fluctuations parallel to the mean flow u' were measured with a single wire about 2 millimeters long.

Mean-speed measurement and equipment.—For measuring mean speed, the constant-resistance method was employed. A description of this method may be found in reference 10. A slight variation of this method was necessary, however, when measuring the profile of the heated-plate boundary layer; namely, the wire was maintained at constant temperature rise above the local air stream. Th measuring instruments consisted mainly of a Wheatsto bridge for obtaining the resistance of the wire and a pote tiometer for measuring the current through the wire or t voltage drop across the wire. This mean-speed apparat with the necessary switching devices, together with t amplifier, was built into one large steel cabinet to minimi electrical pickup.

The amplifier.—A four-stage alternating-current amplifi as described in earlier reports (references 1 and 3) was us to amplify the voltage fluctuations across the hot wir The gain of the amplifier was constant within 2 perce between about 5 and 8,000 cycles per second. A standa inductance-resistance compensation circuit was provid and used in all turbulence measurements.

Traversing mechanism.—A complete investigation of t boundary layer and of transition requires a continuo traverse with the measuring instrument along the plate the direction of air flow and normal to the plate (in t y-direction). The hot-wire carriage as shown in figure 4 constructed of three aluminum legs and a gear train wi micrometer attachment for transporting the hot wire in t y-direction. The carriage is moved along the tunnel on track by a 120-volt alternating-current motor, and t movement in the y-direction is controlled by a 6-volt dire current motor. Switches outside the tunnel enable t operator to control the position of the hot wire in bo directions, and substitution of a glass plate for the usu wooden top panel permits reading of the micrometer givi y-position.

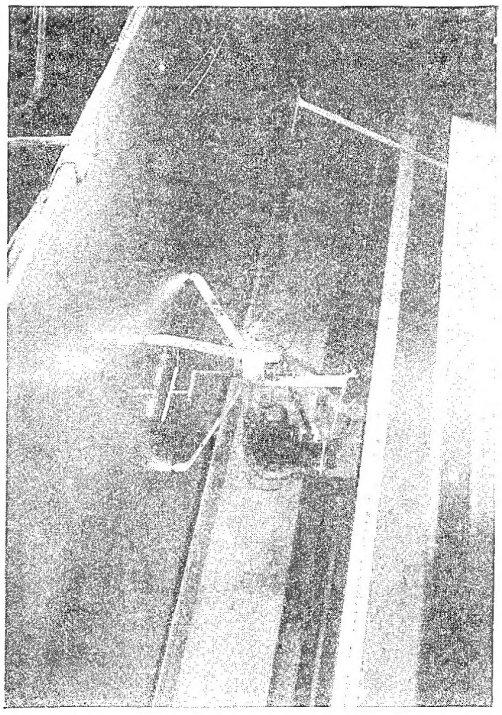

FIGURE 4.—Traversing mechanism.

TURBULENCE LEVEL IN TUNNEL

The turbulence level in the working section is reduced b a honeycomb and a screen in the forward part of the wi tunnel. The honeycomb is at the intake of the tunnel a serves mainly to smooth the very irregular flow entering t tunnel. It is of spot-welded construction, having ½-in cells with a depth of 4½ inches. The screen is located inches behind the honeycomb and is a seamless precisi

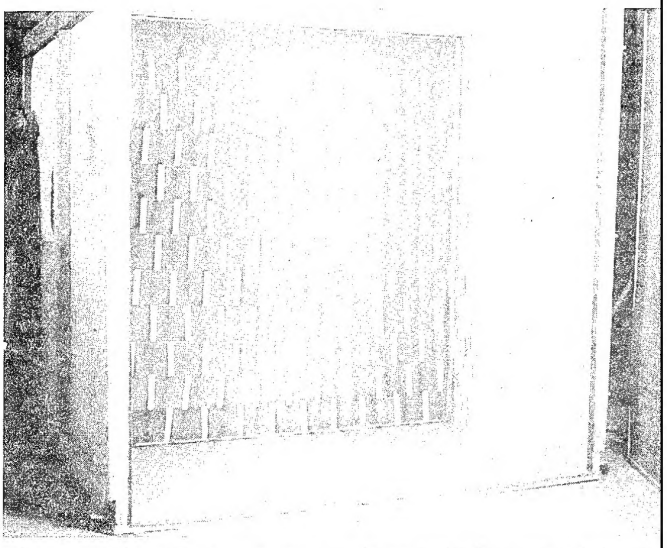

FIGURE 5.—Method of mounting paper strips to create artificial turbulence in tunnel.

screen with 18 mesh per inch and a wire diameter of 0.018 inch. The free-stream turbulence level in this tunnel is

$$\frac{u'}{U_0} \approx 0.0005; \frac{v'}{U_0} \approx \frac{w'}{U_0} \approx 0.0008$$

Artificial turbulence was introduced for one particular phase of the investigation on the heated plate. Strips of notebook paper 1 by 6 inches were strung 6 inches apart on wires just upstream of the screen. The turbulence level in the test section was then determined to be 0.17 percent. Figure 5 shows the method of mounting the paper strips; the honeycomb was rolled away for the picture.

HEATING OF PLATE

The plate was heated by means of Nichrome resistance wires mounted on the back of the flat plate. The elements were more closely spaced near the leading edge since it was evident that for a given wall temperature the rate of heat transfer to the boundary layer would be larger near the leading edge, where the gradients are larger. The temperature of the plate was controlled by grouping the heating elements into four separate circuits and inserting an external variable resistance in each circuit. Thus the temperature gradient along the plate was made nearly zero (see fig. 6) by varying the resistance when the plate temperature had reached equilibrium with the air flowing.

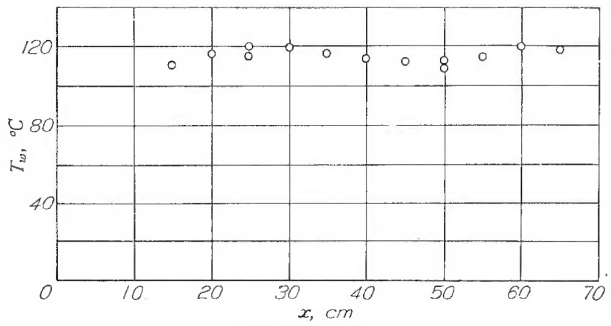

FIGURE 6.—Temperature distribution along heated plate.

The temperature along the plate was determined by a copper-constantan thermocouple mounted in the traversing mechanism. Readings were taken at intervals of 5 centimeters along the plate. Voltages were read with a Leeds and Northrup potentiometer, and the corresponding temperature was obtained from a standard calibration chart. The cold junction was maintained at room temperature. The accuracy of the apparatus was determined to be in the neighborhood of ±½° C. A permanent thermocouple was installed at $x=45$ centimeters for continuous observation of the plate temperature. All heated-plate mean-speed measurements were taken with a plate temperature of 115° ±5° C.

Figure 6 presents the temperature distribution along the heated plate maintained in equilibrium with a free-stream velocity of 8.19 meters per second. Two methods were used to bring the plate to the desired temperature. For the mean-speed and mean-temperature measurements, for which it was desired to obtain equilibrium as rapidly as possible, the current was applied to the heating circuits while the air in the tunnel was still. After approximately 25 minutes, when the plate temperature had reached 120° C, the wind tunnel was turned on and the temperature of the plate was allowed to reach equilibrium with a free-stream velocity of 8.19 meters per second. In the investigation of the effect of heating the flat plate on the location of the transition, the tunnel was operated at the desired free-stream velocity and the variation in the position of early turbulent bursts was noted as the plate heated up to its equilibrium temperature. The temperature as a function of time for heating is shown in figure 7.

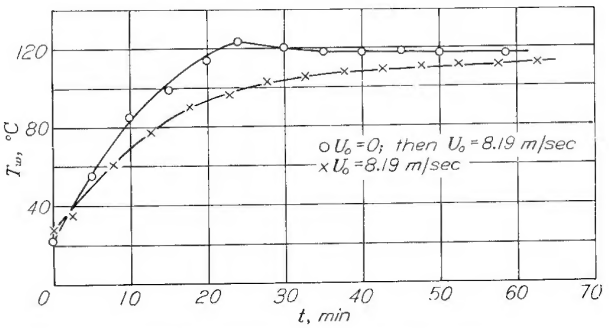

FIGURE 7.—Two methods of heating flat plate.

MEASUREMENT OF PRESSURE DISTRIBUTION

A small total-head tube made from a hypodermic needle and a similar small static tube, mounted together, were used in measuring the pressure distribution along the plate. The total-head tube was a No. 20 gage hypodermic needle flattened to 0.0165 inch in the y-direction, and the static tube was a 1/16-inch-diameter brass tube of standard design. They were mounted in the traversing mechanism just outside the boundary layer. The pressure along the plate was measured with an alcohol manometer at this constant distance. Figure 8 shows the pressure distribution for both roughness and surface-temperature investigations.

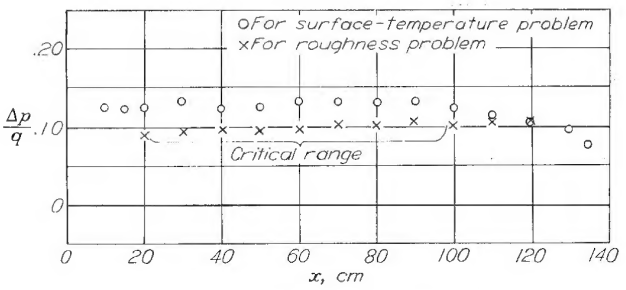

FIGURE 8.—Pressure distribution along test plate.

For the roughness-element tests it was necessary to adjust the side walls only slightly to obtain $\frac{dp}{dx}=0$ and thus to obtain a velocity profile of the Blasius type. The addition of the equipment for heating the plate, however, resulted in a plate thickness of 1½ inches. This finite thickness necessitated tunnel adjustments to preserve Blasius flat-plate flow—that is, to obtain a negligible pressure gradient and to put the stagnation point on the "working" side of the plate.

A transverse screen near the trailing edge of the plate, which increased the resistance to air flow on the working side of the plate, served to solve the problem of pressure gradient. The plate supports were adjusted to give a slightly favorable angle of attack to the plate (approx. $\frac{1}{2}°$). Then, satisfactory Blasius flat-plate flow was obtained as shown in the velocity distribution of figure 9.

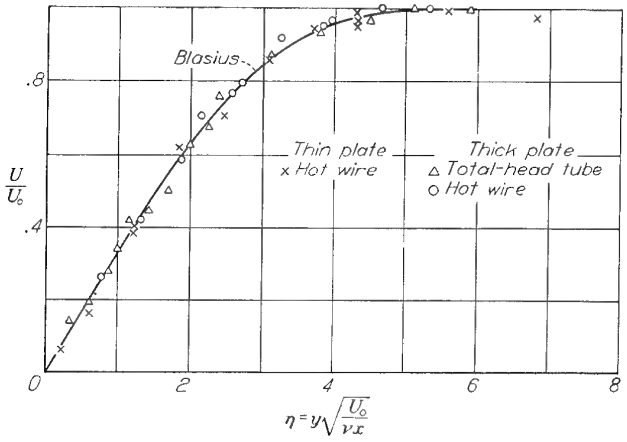

FIGURE 9.—Velocity distribution in boundary layer of unheated flat plate.

DETERMINATION OF TRANSITION POINT

The method used for determination of the beginning of transition was that described in reference 3. This method consists in visual observation of velocity fluctuations measured by a hot-wire instrument and observed on the screen of a cathode-ray oscilloscope. The first appearance of turbulent bursts—that is, occasional sudden changes from a laminar profile to a turbulent profile is taken as the transition criterion.

COMPUTATION OF HEATED-PLATE VELOCITY AND TEMPERATURE PROFILE

For a hot-wire anemometer the relationship between heat loss and airspeed is given by the well-known King equation,

$$H=(A+B\sqrt{U})\theta$$

where θ is the temperature difference between wire and fluid, and A and B are constants for a given fluid.

In general,

$$\theta=\frac{r-r_u}{r_0\alpha}$$

and for steady state, $H=i^2r$. Then there can be written,

$$\frac{i^2r}{r-r_u}=A'+B'\sqrt{U}$$

where $A'=\frac{A}{r_0\alpha}$ and $B'=\frac{B}{r_0\alpha}$.

Both A and B are functions of the absolute temperature of the air, because of appreciable variations in the thermal conductivity and density (reference 11). The mean-velocity calibration of the hot wire was carried out at room temperature and then, in computing velocity profiles, the values were corrected to the temperature of the air at each measuring point.

The temperature distribution was measured by using the hot wire as a resistance thermometer; that is, the "cold" resistances of the hot wire r_u, measured with negligible heating current, give a direct measure of air temperature.

Since

$$r_u=r_f(1+\alpha\theta_u)$$

and

$$r_w=r_f(1+\alpha\theta_w)$$

then

$$\frac{\theta_u}{\theta_w}=\frac{r_u-r_f}{r_w-r_f}$$

In order to get a direct comparison between the velocity and temperature distributions, the following equation is plotted

$$1-\frac{\theta_u}{\theta_w}=\frac{r_w-r_u}{r_w-r_f}$$

MEASUREMENTS AND RESULTS

EFFECT OF SURFACE TEMPERATURE

Mean-velocity distribution.—The mean-speed distribution in the boundary layer of the heated flat plate was measured using both the hot-wire anemometer and the impact tube. During these measurements a peculiar difficulty was encountered. General analytical considerations, discussed in a further section of the report, show that the velocity profile near a heated flat plate should be an inflection-point profile. Also, this type of profile is indicated in the measurements of Frick and McCullough in reference 9. Indeed, the observed velocity profiles generally show this behavior, as is seen in figure 10. The temperature distribution exhibits a behavior very similar to that of the velocity distribution (fig. 11), as is to be expected since the Prandtl number σ for air is close to 1 ($\sigma=0.76$).

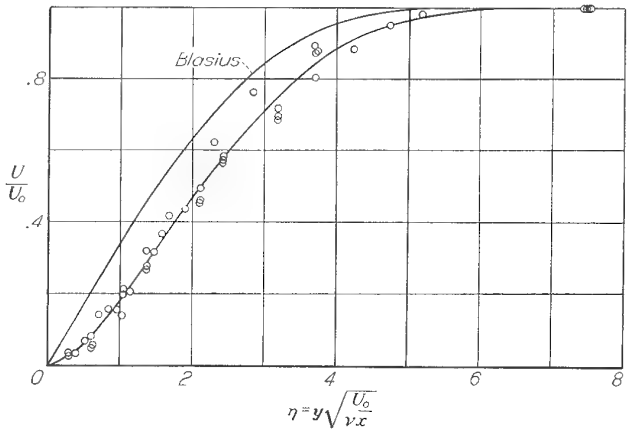

FIGURE 10.—Velocity distribution in boundary layer of heated plate. Regular profile confirming analytical considerations.

On some days, however, no consistent velocity profile could be obtained. In these cases both hot-wire and impact-tube measurements showed a large scatter, and no reasonable profile could be measured. Figures 12 and 13 show a typical set of these measurements. Much time has been spent in efforts to evaluate this effect quantitatively, without much

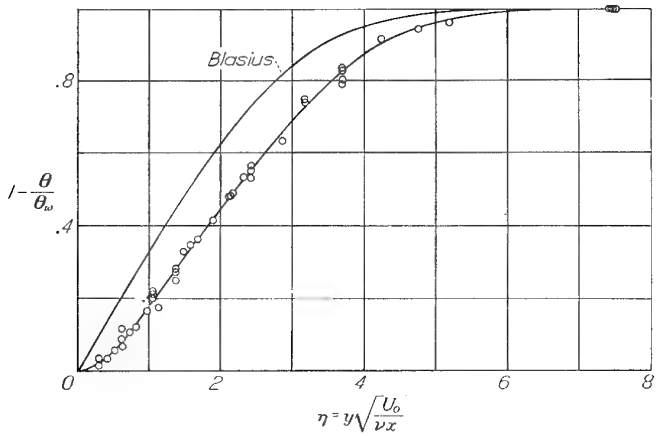

FIGURE 11.—Temperature distribution in boundary layer of heated plate. Regular profile confirming analytical considerations.

success. Qualitatively, the process appears to be as follows: The heated plate was mounted vertically in order to avoid complications in the investigation due to the Prandtl instability, that is, the instability (or stability) due to gravitational effects. The boundary layer of a heated plate mounted vertically is neutrally stable with respect to this Prandtl instability. Gravitational effects will be present, however, so that the heated layers of air close to the surface will have a tendency to rise. This effect probably introduces secondary flow into the boundary layer, especially in the case of a comparatively small tunnel like the one in which the present measurements were made. It is believed that this secondary flow causes the indefinite velocity profiles such as that shown in figure 11. The reasons why these secondary currents occur only a part of the time are not understood. It may well depend upon accidental starting conditions similar to the case in the measurements on rotating cylinders by Pai (reference 12). It is believed that the transition measurements taken at times when the mean-velocity distribution was found normal are not essentially influenced by secondary motion.

Transition point.—The transition point was determined as a function of the surface temperature for two values of the

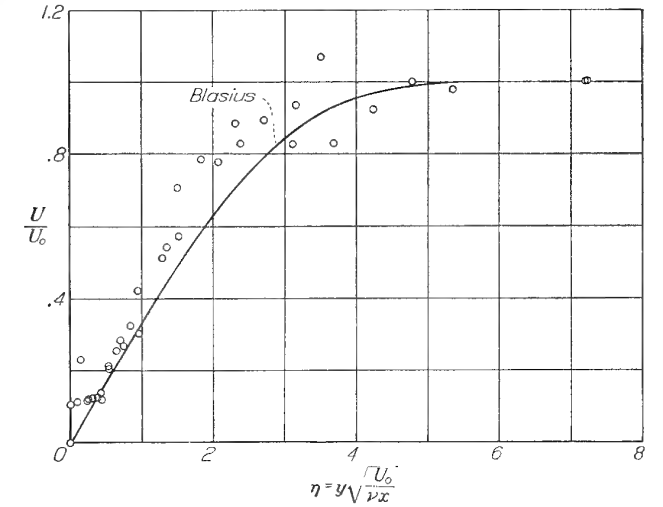

FIGURE 12.—Velocity distribution in boundary layer of heated plate. Unpredicted profile due probably to secondary flow.

831183—49——2

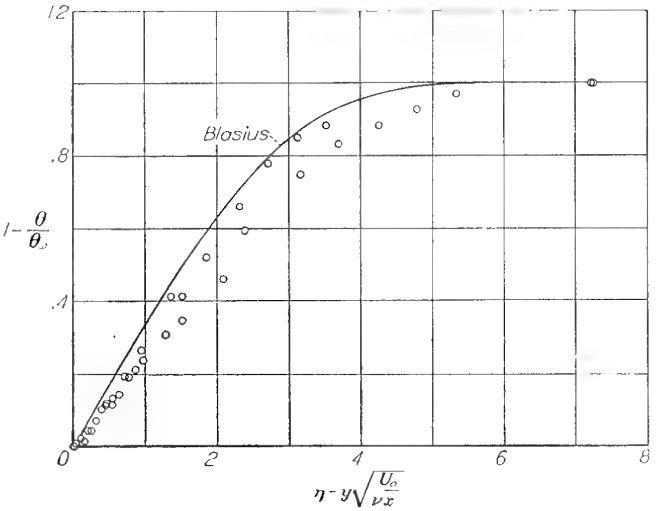

FIGURE 13.—Temperature distribution in boundary layer of heated plate. Unpredicted profile due probably to secondary flow.

free-stream turbulence level, $\frac{u'}{U_0}$=0.05 and 0.17 percent. The results are presented in figure 14, where the distance of the transition point from the leading edge of the plate is plotted as a function of the surface temperature. The effect is obviously quite pronounced; with increasing temperature the transition point moves closer to the leading edge of the plate. The same results are replotted in figures 15 and 16 in terms of Reynolds number of transition against surface temperature.

The kinematic viscosity varies with temperature and thus varies across the boundary layer. It is therefore possible to base the Reynolds number on at least two particular values of the kinematic viscosity, the value at the wall ν_w and that in the free stream ν_f. The Reynolds number of the transition based on ν_f and the Reynolds number based on ν_w are presented as functions of the temperature in figures 15 and 16, respectively. The length used in forming the Reynolds number is in both cases the distance from the leading edge.

The value of R_2 for zero temperature difference between the stream and the plate is very small, considering the low free-stream turbulence level existing in this tunnel. This

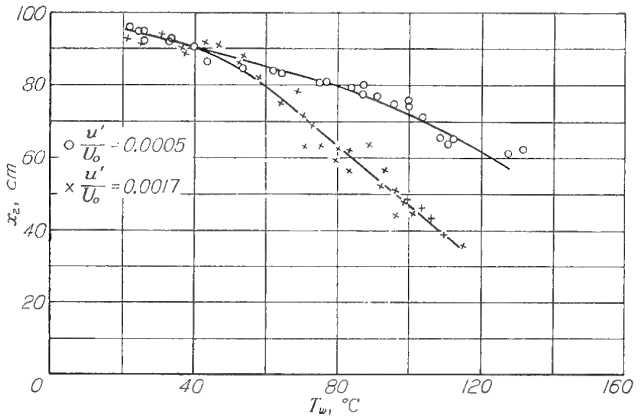

FIGURE 14.—Effect of plate temperature on transition.

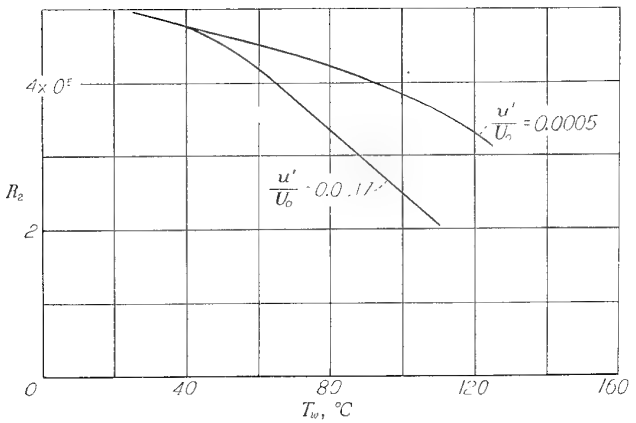

FIGURE 15.—Effect of plate temperature on Reynolds number of transition (ν_T).

small value of R_2 is due to the transverse contamination effect described by Charters (reference 13): The largest possible length, measured from the leading edge, of a laminar boundary layer is limited by contamination from the top and the bottom. Since the measurements had to be carried out at a low velocity (8.19 m/sec) the maximum possible Reynolds number is comparatively small.

EFFECT OF ROUGHNESS ELEMENTS

The mean-speed distributions in the wake of the half-cylindrical roughness elements of ⅛- and 1/16-inch height have been measured with the hot-wire anemometer. The roughness elements were mounted on the flat plate at a distance of 50 centimeters from the leading edge for the investigation of the effect in the laminar boundary layer and at a distance of 140 centimeters from the leading edge for the investigation of the effect in the turbulent layer. Figures 17 and 18 present the results of these measurements in the case where the element is placed in the laminar layer. Three typical cases can be distinguished. At the lowest speed (fig. 17 (a)) the flow, after passing over the roughness element, returned to the surface and continued in the laminar state for some distance downstream. When the velocity was increased, the flow returned to the surface still laminar, but transition occurred almost immediately after the layer reached the surface of the plate (fig. 17 (b)). When the velocity was increased still further, the flow became turbulent in the free

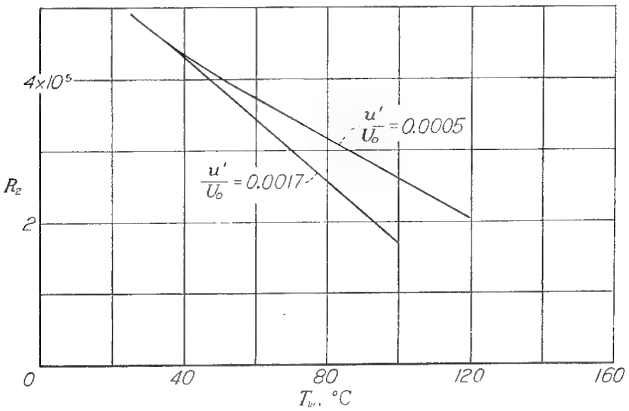

FIGURE 16.—Effect of plate temperature on Reynolds number of transition (ν_w).

boundary layer in the wake of the obstacle (fig. 17 (c)) and returned to the surface in the turbulent state. Figures 18 (a) and 18 (b) show similar effects behind the larger roughness element.

The elements were then placed in the turbulent boundary layer at a distance of 140 centimeters from the leading edge and the mean-velocity profiles again were measured downstream of the element. Figure 19 shows a typical result of these measurements. The velocity distribution in this figure is plotted against the logarithm of the distance from the wall. It is seen that the velocity profile returns rapidly to a "normal" turbulent profile, which is represented, of course, by a straight line in the logarithmic plot.

These experiments are not to be considered as a quantitative investigation. They are intended to show the types of physical phenomena connected with boundary-layer flow past roughness elements. A more complete investigation requires a larger tunnel in which thicker boundary layers can be obtained without introducing secondary flow.

DISCUSSION

MEAN-VELOCITY PROFILE NEAR A HEATED WALL

The laminar-boundary-layer equation in the absence of a pressure gradient for two-dimensional flow past a wall of negligible curvature is

$$\rho U\frac{\partial U}{\partial x}+\rho V\frac{\partial U}{\partial y}=\frac{\partial}{\partial y}\left(\mu\frac{\partial U}{\partial y}\right)$$

if $\mu=\mu(y)$.

If the wall is approached, U and V approach zero and, thus

$$\left[\frac{\partial}{\partial y}\left(\mu\frac{\partial U}{\partial y}\right)\right]_{y=0}=0$$

Hence the curvature of the velocity profile at the wall becomes

$$\left(\frac{\partial^2 U}{\partial y^2}\right)_{y=0}=-\frac{1}{\mu_{y=0}}\left(\frac{\partial\mu}{\partial y}\right)_{y=0}\left(\frac{\partial U}{\partial y}\right)_{y=0}$$

If the surface is heated, the temperature will drop with increasing y. For a gas, μ increases with temperature and consequently,

$$\frac{\partial\mu}{\partial y}<0$$

Since the velocity U increases with y,

$$\frac{\partial U}{\partial y}>0$$

and, thus,

$$\left(\frac{\partial^2 U}{\partial y^2}\right)_{y=0}>0$$

if the surface temperature T_w is higher than the free-stream temperature T_f.

At the edge of the boundary layer, U approaches the constant free-stream velocity U_0 asymptotically and, hence,

Mr. L. Lees has computed the complete temperature and velocity profiles. His results have been published as NACA Rep. No. 876.

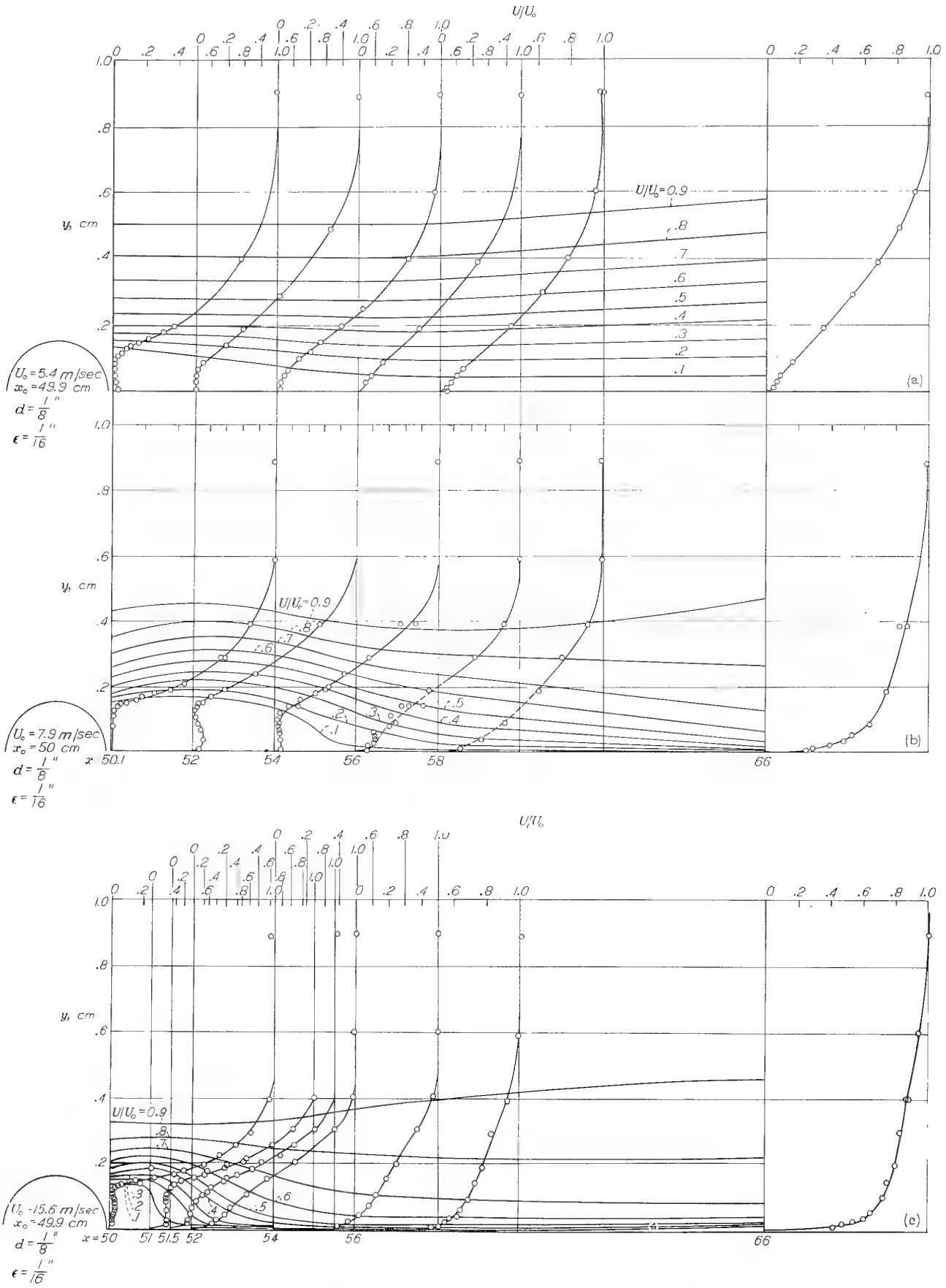

FIGURE 17. Velocity profiles downstream from a small roughness element.

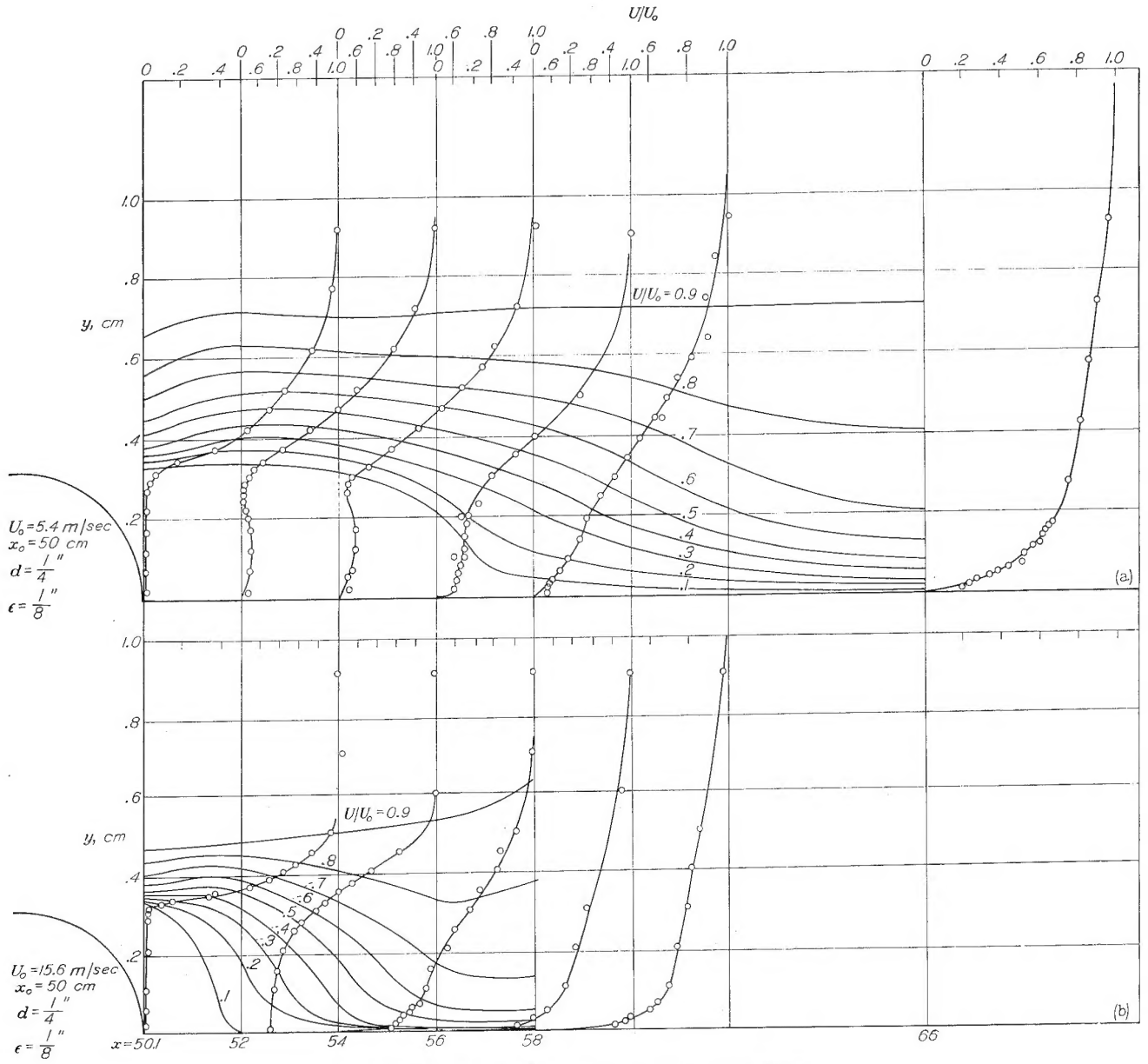

FIGURE 18.—Velocity profiles downstream from a large roughness element.

$$\frac{\partial^2 U}{\partial y^2}<0$$

at the edge of the layer. Consequently,

$$\frac{\partial^2 U}{\partial y^2}=0$$

at some point within the boundary layer.

The effect of surface temperature is similar to the effect of a pressure gradient. In the case of a pressure gradient, and zero temperature gradient, an analogous discussion gives

$$\left(\frac{\partial^2 U}{\partial y^2}\right)_{y=0}=\frac{1}{\mu}\frac{\partial p}{\partial x}$$

and, thus,

$$\left(\frac{\partial^2 U}{\partial y^2}\right)_{y=0}>0$$

if p increases with x, that is, in the case of an "adverse" pressure gradient. Both of these effects are evidently independent of ρ.

INSTABILITY OF INFLECTION-POINT PROFILES

Tollmien (reference 14) obtained the theoretical result that inflection-point profiles are always unstable. Based on this result, inflection-point profiles have been considered as distinguished sharply from normal profiles, that is, profiles with negative curvature throughout. Lin's analysis (reference 4) shows that such a sharp distinction cannot be drawn. Lin shows that a difference in the stability character of normal and inflection-point profiles becomes apparent only for very large Reynolds numbers. The range of wave length of unstable perturbations (see references 2 to 4) tends to zero if the Reynolds number approaches infinity for the normal pro-

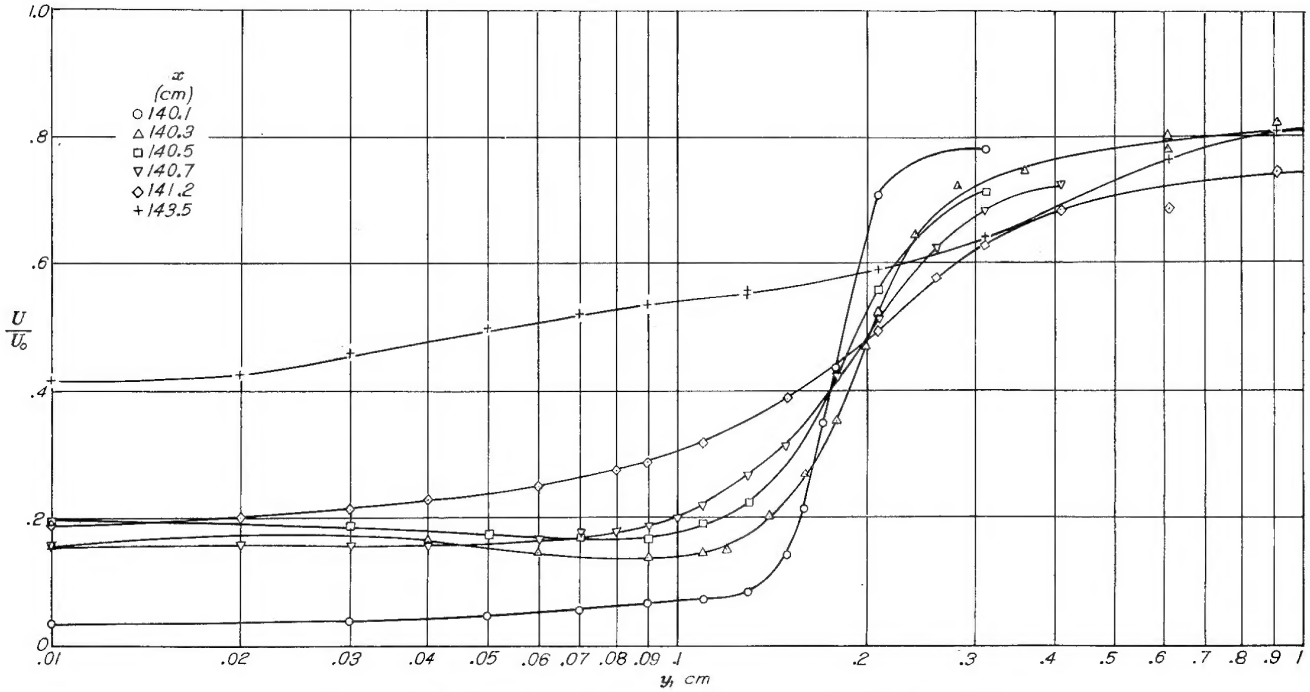

FIGURE 19.—Logarithmic plot of turbulent-velocity profiles downstream from a roughness element.

file, but remains finite as the Reynolds number approaches infinity for the inflection-point profiles. This result is in fact not contradictory to Tollmien, since Tollmien's considerations are restricted to a nonviscous fluid, which simply means the Reynolds number approaches infinity. Lin's considerations do show, however, that the instability of a profile—that is, the critical Reynolds number, the extent of the range of unstable wave length, and so forth—depends on the magnitudes of the slope and of the curvature of the velocity profile near the wall. In fact, it shows that inflection-point profiles generally do have a lower critical Reynolds number and a larger zone of unstable wave length than normal profiles. Consequently, transition in the boundary layer of a gas flow is hastened by an increased surface temperature because inflection-point profiles develop. It is interesting to note that surface temperature should have the opposite effect in a liquid; there the viscosity decreases with increasing temperature, and consequently in the velocity profile of a liquid on a heated surface

$$\left(\frac{\partial^2 U}{\partial y^2}\right)_{y=0} < 0$$

LAMINAR SEPARATION AND TRANSITION

It has been assumed in some earlier considerations of laminar boundary layers that transition sets in immediately at the point of separation. In fact, in attempts to compute and predict transition, it has often been assumed that it is sufficient to show that at some place in the laminar layer a separation profile, that is, a velocity profile which has a normal tangent at the wall, develops.

The results of the surveys in the wake of the obstacles show that the existence of a separation profile does not necessarily lead to transition. In figure 17, for example, the boundary layer is separated from the solid boundary for a considerable distance downstream from the roughness element and still remains laminar, even after reattachment.

A second problem of laminar separation and transition is the following: With the assumption that the boundary layer becomes turbulent in the detached condition (as, for example, in figs. 17 (c) and 18 (c)), determine the velocity profile that exists after the turbulent free layer has reattached to the wall. The measurements (figs. 17 (c) and 18 (b)) show that, in the investigated configuration, the velocity profile transforms very rapidly to a normal turbulent-boundary-layer profile, that is, the logarithmic-type profile. The same rapid transformation to a logarithmic profile also occurs if the element is placed in the turbulent layer (fig. 19).

It should be very interesting to investigate whether a turbulent separated profile always changes to a logarithmic profile as rapidly as in these measurements of flow past a flat plate. For example, the influence of an adverse pressure gradient and of curvature of the solid boundary appears to be of interest in connection with the problem of laminar separation and subsequent reattachment of the boundary layer near the leading edge of airfoils. Problems of this kind are thought to be quite important in connection with the design of sharp-nose airfoils for high-speed flow.

CONCLUDING REMARKS

An increased temperature of the wall hastens boundary-layer transition. This result confirms earlier measurements of Frick and McCullough. In investigating the influence of surface temperature on transition, two effects must be distinguished, an effect due to gravitational forces and an effect due to the dependence of the viscosity of a gas on the temperature. The second effect is the one investigated by the present authors and also by Frick and McCullough. The dependence of the viscosity on the temperature, if the fluid

is a gas, leads to velocity profiles with positive curvature at the wall and therefore to greater instability for a heated wall than for an unheated one. Furthermore, it is confirmed that, even with large deviation from the Blasius condition, the velocity and temperature profiles are very nearly identical, as predictable theoretically for a Prandtl number σ of the order of 1.0 (for air, $\sigma=0.76$).

Studies of air flow in the wake of large, two-dimensional roughness elements show that a laminar boundary layer can separate from the wall and reattach itself without transition taking place. If transition takes place in the detached layer, the velocity profile in the reattached boundary layer will approach the normal turbulent-boundary-layer profile very rapidly.

California Institute of Technology,
Pasadena, Calif., *August 28, 1946.*

REFERENCES

1. Liepmann, H. W.: Investigation of Boundary Layer Transition on Concave Walls. NACA ACR No. 4J28, 1945.
2. Schubauer, G. B., and Skramstad, H. K.: Laminar-Boundary-Layer Oscillations and Transition on a Flat Plate. NACA ACR, April 1943.
3. Liepmann, Hans W.: Investigations on Laminar Boundary-Layer Stability and Transition on Curved Boundaries. NACA ACR No. 3H30, 1943.
4. Lin, Chia-Chiao: On the Development of Turbulence. Quart. Appl. Math., July 1945, Oct. 1945, and Jan. 1946.
5. Fluid Motion Panel of the Aeronautical Research Committee and Others: Modern Developments in Fluid Dynamics. Vol. II, S. Goldstein, ed., The Clarendon Press (Oxford), 1938, pp. 376–380.
6. Prandtl, L.: Einfluss Stabilisierender Kräfte auf die Turbulenz, A. Gilles, L. Hopf, Th. von Kármán, Vorträge aus dem Gebiete der Aerodynamik und verwandter Gebiete (Aachen), 1929.
7. Schlichting, H.: Turbulenz bei Wärmeschichtung. Proc. Fourth Int. Cong. Appl. Mech. (July 3rd–9th, 1934), The Univ. Press (Cambridge), 1935, pp. 245–246.
8. Reichardt, H.: Heat Transfer through Turbulent Friction Layers. NACA TM No. 1047, 1943.
9. Frick, Charles W., Jr., and McCullough, George B.: Tests of a Heated Low-Drag Airfoil. NACA ARR, Dec. 1942.
10. Mock, W. C., Jr., and Dryden, H. L.: Improved Apparatus for the Measurement of Fluctuations of Air Speed in Turbulent Flow. NACA Rep. No. 448, 1933.
11. King, Louis Vessot: On the Convection of Heat from Small Cylinders in a Stream of Fluid: Determination of the Convection Constants of Small Platinum Wires with Applications to Hot-Wire Anemometry. Phil. Trans. Roy. Soc. (London), ser. A, vol. 214, Nov. 12, 1914, pp. 373–432.
12. Pai, Shih-I: Turbulent Flow between Rotating Cylinders. NACA TN No. 892, 1943.
13. Charters, Alex C., Jr.: Transition between Laminar and Turbulent Flow by Transverse Contamination. NACA TN No. 891, 1943.
14. Tollmien, W.: General Instability Criterion of Laminar Velocity Distributions. NACA TM No. 792, 1936.

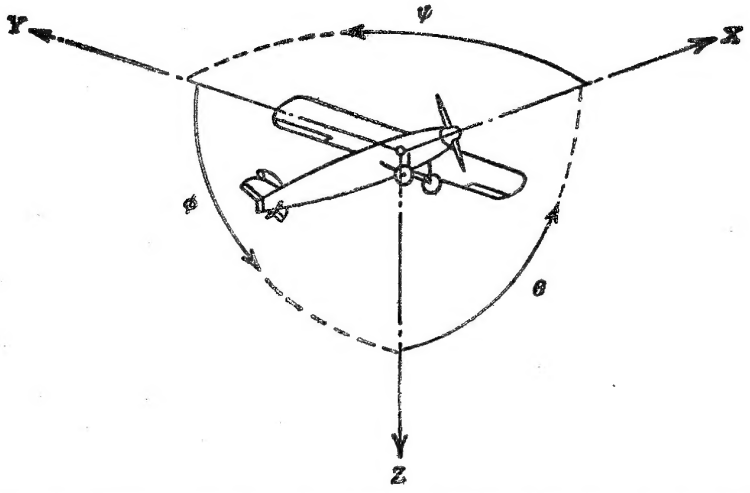

Positive directions of axes and angles (forces and moments) are shown by arrows

Axis		Force (parallel to axis) symbol	Moment about axis			Angle		Velocities	
Designation	Symbol		Designation	Symbol	Positive direction	Designation	Symbol	Linear (component along axis)	Angular
Longitudinal	X	X	Rolling	L	$Y \longrightarrow Z$	Roll	ϕ	u	p
Lateral	Y	Y	Pitching	M	$Z \longrightarrow X$	Pitch	θ	v	q
Normal	Z	Z	Yawing	N	$X \longrightarrow Y$	Yaw	ψ	w	r

Absolute coefficients of moment

$C_l = \frac{L}{qbS}$ (rolling) $\quad C_m = \frac{M}{qcS}$ (pitching) $\quad C_n = \frac{N}{qbS}$ (yawing)

Angle of set of control surface (relative to neutral position), δ. (Indicate surface by proper subscript.)

4. PROPELLER SYMBOLS

D Diameter

p Geometric pitch

p/D Pitch ratio

V' Inflow velocity

V_s Slipstream velocity

T Thrust, absolute coefficient $C_T = \frac{T}{\rho n^2 D^4}$

Q Torque, absolute coefficient $C_Q = \frac{Q}{\rho n^2 D^5}$

P Power, absolute coefficient $C_P = \frac{P}{\rho n^3 D^5}$

C_s Speed-power coefficient $= \sqrt[5]{\frac{\rho V^5}{P n^2}}$

η Efficiency

n Revolutions per second, rps

Φ Effective helix angle $= \tan^{-1}\left(\frac{V}{2\pi r n}\right)$

5. NUMERICAL RELATIONS

1 hp=76.04 kg-m/s=550 ft-lb/sec

1 metric horsepower=0.9863 hp

1 mph=0.4470 mps

1 mps=2.2369 mph

1 lb=0.4536 kg

1 kg=2.2046 lb

1 mi=1,609.35 m=5,280 ft

1 m=3.2808 ft